PROBLEMS OF MECHATRONICS
ARMAMENT, AVIATION, SAFETY ENGINEERING

ISSN 2081-5891

6, 3 (21), 2015, 7-18

Numerical-Experimental Evaluation of the ArmourProtection Capabilities

Adam WIŚNIEWSKI*, Paweł ŻOCHOWSKI

Military Institute of Armament Technology,
7 Wyszyńskiego St., 05-220 Zielonka, Poland
**corresponding author, e-mail: wisniewskia@witu.mil.pl*

Manuscript received July 01, 2014. Final manuscript received February 06, 2015

DOI: 10.5604/20815891.1166972

Abstract. This paper presents a numerical and experimental study of a composite add-on armour panel used for protection of lightweight armoured vehicles impacted by the 7.62 mm API (Armour Piercing Incendiary) BZ projectile (2nd level of International Agreement STANAG 4569). The composite armour consists of a number of ceramic tiles supported by one layer of aramid fabric placed inside an aluminium casing. The problem of the impact of the projectile onto the composite armour has been solved in three-dimension space (3D) with the use of CAD and CAE methods implemented in Ansys Autodyn v15 software. On the basis of the results of computer simulations, the proportions of the thickness of the armour layers were chosen. After that, the real model of the composite armour was built and tested in the firing range. The results obtained in the simulations were compared with the depth of penetration (*DP*) tests results, and satisfying agreement was obtained.

Keywords: mechanics, composite armour, 7.62 mm API BZ projectile, numerical simulation

This paper is based on the work presented at the 10th International Armament Conference on „Scientific Aspects of Armament and Safety Technology", Ryn, Poland, September 15-18, 2014.

1. INTRODUCTION

Light armoured vehicles are usually used to transport soldiers in the conflict areas. Vehicles are equipped with the main armour (made either of steel or aluminium and usually fixed to the hull). The main function of the armour is to protect troops inside and vehicle against the damage or destruction in consequence of perforation with the projectile fired in its direction. The protection level (thickness) of the main armour usually differs for the every part of the vehicle.

Enhancement of the protection level of a vehicle requires adding to the main armour the add-on armour, usually in the form of panels which are screwed to the hull. The advantage of the additional construction is that the damaged panels can be quickly either replaced by new ones or repaired. The traditional add-on armours of the light armoured vehicles (LAVs) are monolithic, often made of a high strength steel plate. Recently, one can observe increasing requirements for the armour systems that can provide maximum ballistic protection at minimum weight. Since the add-on armour causes increase in the vehicle weight and reduction of its mobility, it is important to reach a compromise between the weight and the protection capacity of the vehicle.

For this purpose the composite armours, e.g. the ceramic-metal armours, are widely applied as protection of light weight vehicles, helicopters and airplanes. The penetration process of this type of armours with the AP projectiles is complex and has been studied by many researchers.

Due to the complexity of these phenomena, analysis of these types of protection systems requires interdisciplinary approaches, from which the most commonly used methods are:

1. analytical modelling;
2. numerical simulation;
3. empirical methods.

The analytical models are based on the equations describing the penetration processes. They are derived from the continuum mechanics laws and are usually valid for one specific projectile-armour system and cannot be used for other systems. One of the earliest analytical analyses of the penetration mechanics of composite armours was described in the works by Wilkins [1] and Florence [2] where the authors developed analytical models for the two-component armour. In the work by Goncalves et al. [3], the author presented a model allowing calculation of the decrease in the projectile mass and velocity, as well as the deflection of the backup material for the impact against the ceramic-metal armour.

Numerical simulations are widely used for armour design optimization. In ref. by Mei et al. [4], the LS-DYNA FE code was used to simulate the projectile penetration against the target plate with different ceramic-steel thickness ratios.

In Feli et al. [5] LS-DYNA FE code was also used to simulate the perforation of the ceramic-composite armours, impacted by cylindrical tungsten projectiles. In Sánchez et al. [6], the author summarized the application of analytical and numerical computations of the ceramic-metal and ceramic-composite add-on armour failure processes as valuable tools for armour design optimization.

LS-DYNA FE code was also used in Stanisławek et al. [7] to numerically study a two-layer composite panel, made of a number of pyramid ceramic components supported by an aluminium plate, impacted by a 14.5×118 mm B32 projectile. Numerical codes and mainly finite element method (FEM) are used to solve the equations describing the impact process. With these methods one can obtain lots of useful information: stresses, strains, velocities and accelerations at different points of the projectile and the target in function of time, etc. The main disadvantage of the described methods is the lack of available data describing the material behaviour i.e., parameters which determine the material's failure and strengthening mechanisms. As a result, in an armour designing process it is often necessary to run experimental tests to determine the dynamic properties of the materials.

The empirical methods are usually based only on the depth of penetration tests. This procedure for armour design optimization is very expensive because every single armour variant requires construction of a prototype. The information obtained during the tests is limited in comparison to simulations, and is valid only for a specific projectile-armour system.

In this article a design of a multi-layered add-on armour consisting of an aluminium alloy plate, ceramic tiles, and aramid fabric is presented and its protection effectiveness is evaluated both in numerical and empirical ways. The designed armour was expected to protect against the projectiles of the 2nd level of International Agreement STANAG 4569, and was intended to be placed on a LAV with the main armour made of 4-6 mm of 500 HB steel plate.

2. CONSTITUTIVE MODEL OF METAL AND CERAMIC MATERIALS

This paper presents a numerical study of a multi-layer composite add-on armour impacted by the 7.62 API BZ projectile. The problem has been solved with the use of the finite element method and Ansys Autodyn v15 software. For the simulation of the material behaviour, specific material models including constitutive relations, strengthening and failure mechanisms were chosen. Materials of the projectile, steel and the aluminium plates were described by the Johnson–Cook model. Ceramic tiles were described by the Johnson–Holmquist model.

The Johnson–Cook strength model is expressed with the equations:

$$\sigma_y = \left(A + B\bar{\varepsilon}^{p^n}\right)(1 + cln\dot{\varepsilon}^*)(1 - T^{*m}) \tag{1}$$

$$\dot{\varepsilon}^* = \frac{\dot{\bar{\varepsilon}}^p}{\dot{\varepsilon}_0} \tag{2}$$

$$T^* = \frac{T - T_{room}}{T_{melt} - T_{room}} \tag{3}$$

where: A – yield strength, B – hardening constant, n – hardening exponent, C – strain rate constant, m – thermal softening exponent, ε – strain, $\bar{\varepsilon}^p$ – equivalent plastic strain, $\dot{\bar{\varepsilon}}^p$ – plastic strain rate, $\dot{\varepsilon}^*$ – dimensionless plastic strain rate, $\dot{\varepsilon}_0$ – effective plastic strain rate of the quasi-static test used to determine the yield and hardening parameters, T^* – non dimensional temperature, T_{room} – reference temperature, T_{melt} – melt temperature, T – temperature during determination of the yield and hardening parameters.

The Johnson–Holmquist model is a pressure and strain-rate sensitive material model used for constitutive modelling of the dynamic brittle failure and damage evolution of the ceramics. This model consists of a polynomial equation of state, which evaluates the current state of pressure as a function of the volumetric change. A specific feature of this model is the use of two strength limits of the material, one for intact and one for the fractured material. Both values are described by the pressure p and the strain rate $\dot{\varepsilon}$.

The constitutive model consists of three parts – strength, pressure and damage. The Johnson–Holmquist strength model is expressed with the following equations:

1. for intact material:

$$\sigma_i(p,\dot{\varepsilon}) = A_{J-H}\sigma_{HEL}\left(\frac{T+p}{p_{HEL}}\right)^{N_{J-H}}\left(1 + C_{J-H}\ln\left(\frac{\dot{\varepsilon}}{\dot{\varepsilon}_0}\right)\right) \tag{4}$$

2. for fractured material:

$$\sigma_f(p,\dot{\varepsilon}) = B_{J-H}\sigma_{HEL}\left(\frac{p}{p_{HEL}}\right)^{M_{J-H}}\left(1 + C_{J-H}\ln\left(\frac{\dot{\varepsilon}}{\dot{\varepsilon}_0}\right)\right) \tag{5}$$

- failure model equation:

$$\varepsilon_p^f(p) = D_1\left(\frac{T+p}{p_{HEL}}\right)^{D_2} \tag{6}$$

where: p_{HEL} – pressure at Hugoniot elastic limit, σ_{HEL} – stress at Hugoniot elastic limit, $A_{J\text{-}H}$ – intact strength constant, $N_{J\text{-}H}$ – intact strength exponent, $C_{J\text{-}H}$ – strain rate constant, $B_{J\text{-}H}$ – fractured strength constant, $M_{J\text{-}H}$ – fractured strength exponent, D_1, D_2 – coefficient and exponent of fracture.

3. PROBLEM DESCRIPTION

The multi-layer composite add-on armour was of 9 mm total thickness and of 250×250 mm size. Full three-dimension models of the projectile and the target were built. A ceramic layer of the armour was made of 6 mm thick ceramic tiles backed with one layer of aramid fabric and placed inside an aluminium casing of 1.5 mm in thickness. The add-on armour was screwed by four bolts on the surface of the main armour, i.e., a 4 mm steel plate. The model is shown in Figure 1.

Both FEM models were built from brick elements only. To increase the accuracy of the simulations, the mesh of the armour was refined in the area from the projectile impact to of the element edge of 0.25 mm in size. The backing plate was supported near its edges. The Ansys Autodyn v15 software was used to solve the problem with the explicit time integration method.

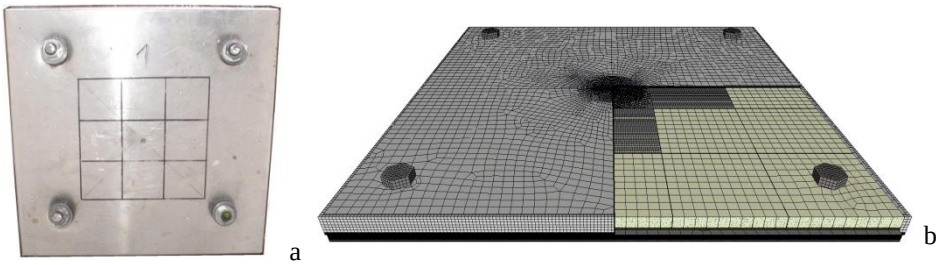

a b

Fig. 1. Analyzed add-on armour:
a – real model, b – discretized numerical model used in simulations

The 7.62 mm API BZ projectile used in the simulations is shown in Figure 2. This kind of projectile is used against light armoured targets. It consists of a tombac plated steel jacket, tombac cap, lead filler, hard steel core and a bowl with the incendiary material placed behind the core. The initial velocity of the projectile amounts to 695 m/s, what equals an impact energy of $E = 2$ kJ. The parameters of the material used in the simulations are listed in Tables 1 and 2.

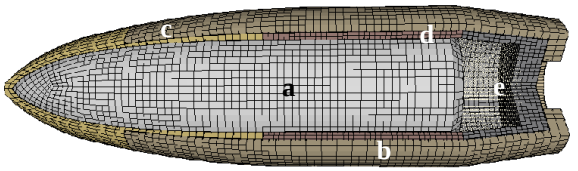

Fig. 2. The 7.62 mm API BZ projectile:
a – steel core
b – tombac plated steel jacket
c – tombac cap
d – lead can
e – incendiary material

Table 1. Parameters of the Johnson–Cook strength and failure models for the materials used in the simulations

Material	ρ, g/cm^3	A, GPa	B, GPa	C	n	m	$D1$	$D2$	$D3$	$D4$	$D5$
Jacket	7.89	0.448	0.3034	0.0033	1.15	1.03	2.25	0.0005	-3.6	-0.0123	0
Lead	10.66	0.0103	0.041	0.0033	0.21	1.03	0.25	0	0	0	0
Armox 500T	7.85	1.47	0.702	0.0054	0.199	0.81	0.068	5.328	-2.554	0	0
Aluminium	2.47	0.435	0.343	0.01	0.41	1	0.059	0.246	-2.41	-0.015	0
Core steel	7.85	1.576	2.906	0.075	0.1172	1.17	Principal Stress = 2.6 GPa				

Table 2. Parameters of the Johnson–Holmquist strength and failure models for the materials used in the simulations

	ρ, g/cm^3	A	B	C	M	N	HEL, GPa	$D1$	$D2$	HTL, GPa
Al_2O_3	3.89	0.88	0.45	0.007	0.6	0.64	7.81	0.012	0.7	-0.262
B_4C	2.51	0.99	0.5	0.03	1	0.77	12.5	0.1	1	-7.3
	ρ, g/cm^3	S_1, GPa	P_1, GPa	S_2, GPa	P_2, GPa	C	HEL, GPa	EF_{max}	P_3, GPa	HTL, GPa
SiC	3.22	7.1	2.5	12.2	10	0.009	11.7	1.2	99.7	-0.75

4. NUMERICAL SOLUTION OF THE PROBLEM

Simulations of the impact of the 7.62 mm API BZ projectile into the layered add-on armour were carried out. The individual layers of the armour were built of materials with properties chosen on the basis of the armour penetration process stages. The layered construction of the add-on armour allowed to use advantageous properties of several materials simultaneously and to reach higher mass efficiency in relation to monolithic steel armours. The areal density of investigated add-on armour was:

1. 32 kg/m^2 for the armour with the Al_2O_3 ceramic tiles
2. 27 kg/m^2 for the armour with the SiC ceramic tiles
3. 23 kg/m^2 for the armour with the B_4C ceramic tiles.

The properties of the ceramic materials investigated in this work and their ballistic efficiency coefficient M determined by equation 7 [8] are shown in Table 3.

$$M = \frac{E \cdot H_k \cdot R_m \cdot T_m}{\rho} \tag{7}$$

where: M – ballistic efficiency coefficient (GPa m)^3 K/kg, E – elastic modulus GPa, H_k – Knoop hardness GPa, R_m – ultimate tensile strength MPa, T_m – melting temperature K, ρ – density g/cm^3.

Table 3. Properties of the ballistic ceramics in relation to RHA [8]

Material	ρ, g/cm^3	H_k, GPa	R_m, MPa	E, GPa	T_m, K	M, (GPa m)^3 K/kg
Al_2O_3	3.9	18	370	390	2320	1.5 10^3
SiC	3.1	21	200	410	3300	1.8 10^3
B_4C	2.5	30	300	450	3300	5.3 10^3
Armour steel	7.8	3.5	3000	210	1950	0.5 10^3

The simulation results of the penetration of the add-on armour with the 7.62 mm API BZ projectile are shown in Figures 3-5.

Figure 6 shows the velocity of the projectile obtained from the simulations as a function of time for armours with different ceramic tiles. In Figure 7, the ballistic effectiveness of the materials is plotted against the cost of the relative ceramics to the RHA steel.

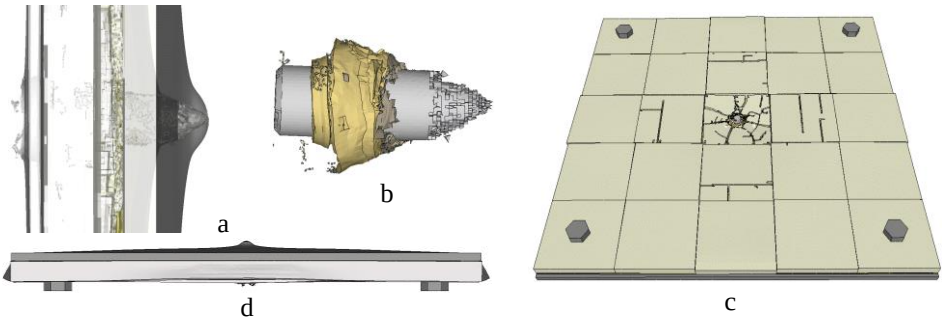

Fig. 3. Simulation results for the armour with Al_2O_3 ceramic tiles:
a – depth of penetration, b – projectile after the shot, c – ceramic layer after the shot, d – bulging of the armour

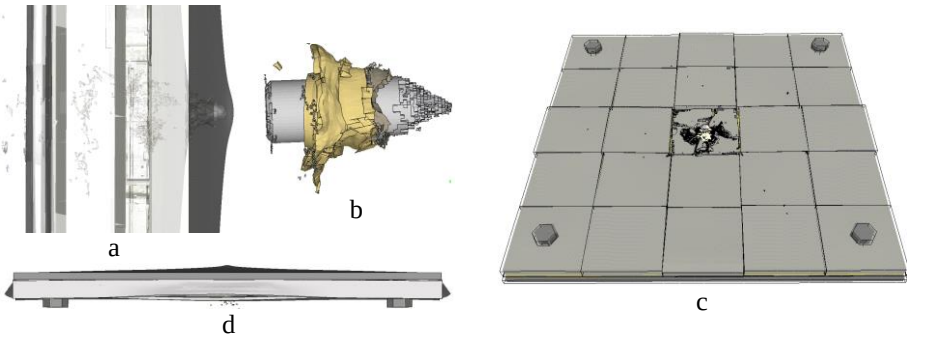

Fig. 4. Simulation results for the armour with SiC ceramic tiles:
a – depth of penetration, b – projectile after the shot, c – ceramic layer after the shot,
d – bulging of the armour

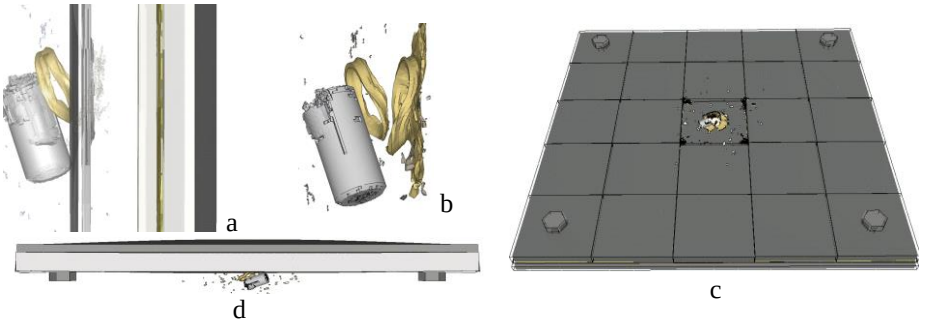

Fig. 5. Simulation results for the armour with B_4C ceramic tiles:
a – depth of penetration, b – projectile after the shot, c – ceramic layer after the shot,
d – bulging of the armour

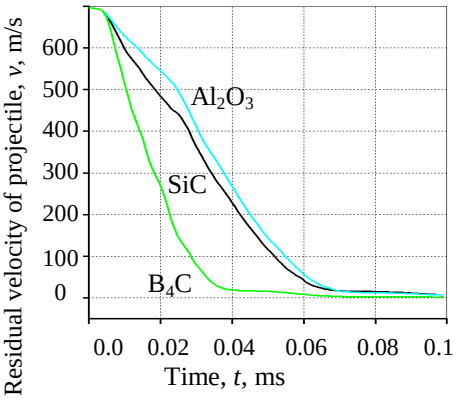

Fig. 6. Velocity of the projectile obtained from the simulations as a function of time for armours with different ceramic tiles

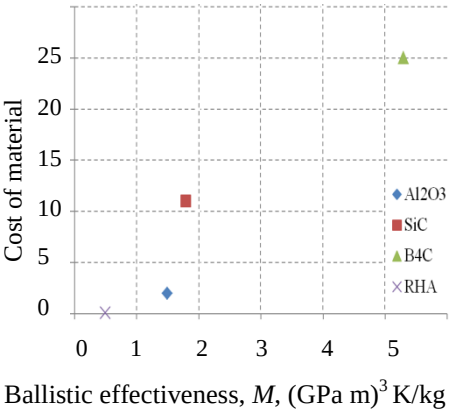

Fig. 7. Ballistic effectiveness vs. costs of the ceramics relative to the RHA steel

Performing the computer simulations allowed making more accurate analysis of the phenomena appearing during the projectile penetration process into the armour than would be possible in the case of experimental research.

In the first stage of the simulation, the projectile hits the armour and a compressive shock wave is generated, travelling in the impact direction. The high yield strength and impedance of the ceramic layer cause fracturing of the projectile nose and partial dissipation of the moment carried by the projectile. When the compressive wave reaches the back surface of the ceramic tiles, it is reflected back as a wave of tension. As a consequence, cracks are formed in the ceramic layer in the form of a cone.

The velocity of the front part of the projectile is much lower than that of the rear part. This difference in velocities causes the growth of compressive stresses in the projectile, and in consequence its erosion.

In the second stage the projectile penetrates the armour with a relatively constant speed. The fragments of the ceramics are pushed in the radial direction and elastic deformation of the armour base begins. The nose of the projectile erodes, which causes the growth of stresses on its length and a little deflection of the projectile from the initial penetration axis. During the penetration into the aluminium layer, the cracks in the penetrator grow and its fragmentation begins.

The use of the orthotropic aramid fabric material as one of the layers limits the propagation of the shock wave in the direction of the penetration, allowing only propagation perpendicular to the direction of penetration. Another function of the aramid fabric layer is to limit the fragmentation ratio of the ceramics.

In the last stage of the penetration process, the projectile penetrates the main armour of the vehicle, i.e., the steel plate. The residual kinetic energy of the projectile and the ceramic fragments are absorbed by the vehicle main armour, the penetrating projectile causes a change in the plastic deformation mode of the armour backing material from indentation to bulging. At this stage further destruction of the projectile and deceleration of its speed appears. In the final stage of the penetration process, tensile stresses appear in the projectile instead of the earlier appearing compressive stresses, which causes further fragmentation of the penetrator.

The analysis of the numerical simulation results showed that the very hard (> 60 HRC) core of the 7.62 mm API BZ projectile is sensitive to the quickly changing stresses, which appear in the use of proper armour constructions.

5. FIRING TESTS

The passive composite add-on armours containing aluminium alloy layers, ceramic tiles and aramid fabric of 250 × 250 mm size were tested also by firing. The depth of penetration *DP* tests were carried out only for the armour variant with the ceramic tiles made of alumina Al_2O_3. The areal density of the armour was 36 kg/m^2.

The tests were performed according to International Agreement STANAG 4569 – level 2 (7.62 API BZ projectile with initial velocity 685 ± 20 m/s) at the angle $\alpha_{NATO} = 0°$ from the normal to the surface of the armour. The testing stand and elements of the tests are shown in Figure 8.

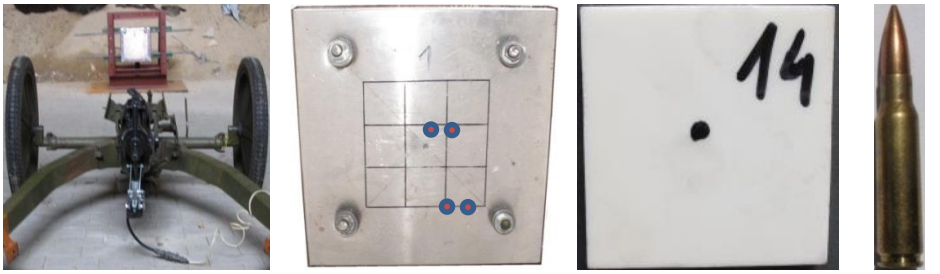

a b c d

Fig. 8. The elements of the tests: a – testing stand, b – places of shots during the „multi hit" shots, c – Al_2O_3 ceramic tile of the armour, d – 7.62 mm API BZ projectile

The tests showed that the analysed armours were efficient enough to protect the main armour of the vehicle, i.e. a steel plate of 4-6 mm thickness, against perforation both in single and multi-hit procedures according to the International Standard AEP55 [9].

The mounting system (bolts and other elements) fixing the add-on armour to the main steel armour was also tested, and it demonstrated sufficient protection efficiency against the projectile.

During the tests, the protection efficiency of the edge area between two joining panels was also examined. The protection efficiency did not decrease, and the results of these tests were similar to the results obtained by shooting at the centre of the panels.

6. CONCLUSIONS

On the basis of the literature analysis, computer simulations and experimental tests, the following conclusions have been drawn:

1. Use of the add-on armour is a good method to improve the protection level of light armoured vehicles against projectile impact.
2. Combination of analytical, numerical and experimental methods is the best way for armour design optimization.
3. Combination of ballistic ceramics and a hard backing (steel and aluminium alloys) is an advantageous solution for the add-on armour.
4. Numerical simulations of the add-on armour penetration processes often require experimental tests to determine the constants in the constitutive equations of the used materials.

5. The tested armours could protect the main armour of the vehicle (a 4-6 mm thickness steel plate) against perforation both in single and multi-hit procedures conducted according to the International Standard AEP55.
6. The mounting system (bolts and other elements) fixing the add-on armour to the main armour of the vehicle showed proper protection efficiency against the projectile.
7. The protection efficiency of the armour in the edge area between two joining panels was similar to the protection efficiency of the armour at the centre of the panels.
8. Use of SiC ceramics instead of Al_2O_3 decreases the mass of the armour by 16% with similar protection efficiency but increases the costs by up to 300%.
9. The B_4C ceramics give much higher protection efficiency than Al_2O_3 and much thinner plates made of B_4C ceramics can be used. Use of the B_4C tiles with the same thickness decreases the weight of the armour by 28%, compared with the Al_2O_3 tiles but increases the cost of the armour by up to 700%.

REFERENCES

[1] Wilkins M.L., Mechanics of penetration and perforation, *International Journal of Engineering Science,* 16, pp. 793-807, 1978.
[2] Florence A.L., *Interaction of Projectiles and Composite Armour Part II,* Standford Research Institute Menlo Park California AMMRC-CR-69-15, August 1969.
[3] Goncalves D.P., De Melo F.C.L., Klein A.N., Al-Qureshi H.A., Analysis and investigation of ballistic impact on ceramic/metal composite armour, *International Journal of Machine Tools & Manufacture*, 44, pp. 307-316, 2004.
[4] Mei H., Wang Y.C., Liu X., Cao D.F., Liu L.S., Numerical investigation on anti-penetration behavior of ceramic/metal target under ballistic impact, *Journal of Physics: Conference Series*, 419 012054, 2013.
[5] Feli S., Asgari M.R., Finite element simulation of ceramic/composite armor under ballistic impact, *Composites: Part B*, 42, pp. 771-780, 2011.
[6] Sánchez Gálvez V., Sánchez Paradela L., Analysis of failure of add-on armour for vehicle protection against ballistic impact, *Engineering Failure Analysis*, 16, pp. 1837-1845, 2009.
[7] Stanisławek S., Morka A., Niezgoda T., Numerical analysis of a multi-component ballistic panel, *Journal of KONES Powertrain and Transport*, vol. 19, no. 4, 2012.

[8] Starczewski L., Współczesne materiały na osłony pancerne, kryteria oceny i metody badań, *Opracowania monograficzne V Konferencji Naukowo-Technicznej „Perspektywy Rozwoju Krajowej Produkcji Napędów Rakietowych oraz Amunicji Strzeleckiej i Artyleryjskiej*, Kołobrzeg, 2011.
[9] International Standard AEP55.